Chinese Chemical Letters 37 (2026) 110893

Contents lists available at ScienceDirect

Chinese Chemical Letters

journal homepage: www.elsevier.com/locate/cclet

Synergy of constructing robust hybrid interphase and weakly solvating electrolyte for low-temperature aqueous zinc-ion batteries

Wen Liu[a,b], Qiwen Zhao[b], Hongli Qi[c], Dongping Chen[c], Fengcheng Tang[b], Xiaoyu Liu[b], Huaming Yu[a,*], Gang Zhou[a,*], Yuejiao Chen[b], Libao Chen[b]

[a] School of Materials Science and Engineering, Dongguan University of Technology, Dongguan 523808, China
[b] State Key Laboratory of Powder Metallurgy, Central South University, Changsha 410083, China
[c] School of Chemistry and Chemical Engineering, Harbin Institute of Technology, Harbin 150001, China

ARTICLE INFO

Article history:
Received 9 December 2024
Revised 14 January 2025
Accepted 20 January 2025
Available online 21 January 2025

Keywords:
Weakly solvating electrolyte
Low-temperature batteries
Aqueous zinc-ion batteries
Low polarity co-solvent
Zn anode

ABSTRACT

Aqueous zinc-ion batteries (AZIBs) have emerged as strong contenders for large-scale energy storage solutions, attributed to their cost-effectiveness and enhanced safety profiles. Nevertheless, their widespread adoption is currently hindered by their poor performance in low-temperature conditions. Herein, an electrolyte is developed by utilizing weakly solvated and film-forming molecule dimethyl sulfite (DMS) to achieve smooth de-solvation and high ionic conductivity at low temperature. The DMS disrupts the hydrogen bonding network of water and lowers the freezing point of the electrolyte to -40.9 °C. The designed electrolyte achieves ionic conductivity up to 10.75 mS/cm at -30 °C. Due to the chemical reactivity of DMS and trifluoromethanesulfonate anions in the Zn^{2+}-solvation shell, a ZnF_2-ZnS hybrid solid electrolyte interphase (SEI) is successively generated on Zn metal surface. Mechanistic studies reveal that such robust hybrid interphase can promote Zn^{2+} desolvation and rapid Zn^{2+} transport. In addition, the addition of DMS effectively suppresses the dendritic growth, hydrogen evolution reaction (HER), and corrosion-induced passivation on the anode surface, facilitating long-term cycling at subzero temperatures. At -40 °C, the Zn//Zn symmetrical cell cycles for 1200 h at 0.5 mA/cm^2 and 0.5 mAh/cm^2, and the Zn//NVO cell achieves an ultra-long cycle life of 1000 cycles with a high capacity retention of 82.89 % at 1 A/g.

© 2026 Published by Elsevier B.V. on behalf of Chinese Chemical Society and Institute of Materia Medica, Chinese Academy of Medical Sciences.

Due to the intermittency and instability of existing renewable energy sources, such as wind, solar, and tidal energy, the development of grid-scale energy storage technologies is necessary [1–4]. The high cost and safety issues of lithium-ion batteries currently being widely used limit their application in the field of energy storage [5–8]. Aqueous zinc-ion batteries (AZIBs) have emerged as appealing choices for economical and large- scale energy storage systems, due to their high safety, low manufacturing costs, and the inherent advantages of Zn metal, including a low redox potential (−0.76 V *versus* the standard hydrogen electrode) and a high theoretical capacity (820 mAh/g and 5855 mAh/cm^3) [9–11]. However, rampant dendrite growth and uncontrollable interfacial corrosion lead to poor cycle performance in AZIBs. Moreover, in stationary energy storage deterioration of the electrode/electrolyte interphase and a decline in ionic transport performance, causing severe performance degradation of the batteries at low temperatures, and even preventing them from functioning [12–14]. This significantly limits the application of AZIBs as next generation of commercial large-scale energy storage systems under various climatic conditions.

As the temperature decreases, the hydrogen bonds between water molecules become stronger, leading to a transition of the hydrogen bond network from short-range to long-range, which causes the electrolyte to solidify and hinders ion transport [15,16]. Additionally, Zn metal is in a thermodynamically unstable state in aqueous electrolytes, which results in continuous and slow H_2 reactions at low temperatures. Specifically, during the zinc electrodeposition process, the desolvation of hydrated zinc ions releases a large number of active water molecules which adsorb onto the anode [17]. Water molecules can compete with Zn^{2+} cations to capture electrons, producing H_2 and causing passivation on the electrode surface. Secondly, free water molecules in the electrolyte form a continuous hydrogen bond network, and under the action of the Grotthuss diffusion mechanism, protons rapidly transfer, accelerating corrosion and hydrogen evolution reaction (HER) at the anode surface [18,19]. The aforementioned processes lead to an

* Corresponding authors.
E-mail addresses: hmYu147@outlook.com (H. Yu), zhougang1986@dgut.edu.cn (G. Zhou).

https://doi.org/10.1016/j.cclet.2025.110893
1001-8417/© 2026 Published by Elsevier B.V. on behalf of Chinese Chemical Society and Institute of Materia Medica, Chinese Academy of Medical Sciences.

increase in local OH^- concentration, which in turn forms a loose, flaky passivation film on the surface of Zn metal, reducing the kinetics of Zn^{2+} transport and leading to uncontrolled growth of zinc dendrites. Therefore, a stable electrolyte system and solid electrolyte interphase (SEI) play a crucial role in both charge transfer and mass transport processes, especially for batteries operating at low temperatures [20,21]. Thus, adjusting the electrolyte composition to break the hydrogen bonds between water molecules and construct a dense and robust SEI on the Zn metal anode surface which can prevent the penetration of water molecules is a key prerequisite for achieving outstanding cycling stability under low-temperature conditions. There is an urgent need for electrolytes with low freezing points, weak solvation affinity, high ionic conductivity, and excellent film-forming characteristics to meet the requirements of long-term reversible cycles for AZIBs at low temperatures.

Herein, we formulate a weakly solvating electrolyte by introducing dimethyl sulfite (DMS) as a cosolvent into 1 mol/L zinc trifluoromethanesulfonate ($Zn(OTf)_2$) to build anti-freezing and long-life AZIBs. The DMS co-solvent not only disrupts hydrogen bonds, conferring a low freezing point of −40.9 °C to the hybrid electrolyte, but also diminishes the quantity of solvated H_2O and water activities. Furthermore, DMS preferentially adsorbs onto the zinc metal anode, undergoing preliminary reduction on the surface, thus creating a robust hybrid SEI containing both ZnS and ZnF_2. Both experimental data and calculation results demonstrate that DMS modulates the internal solvation structure and enhances the desolvation kinetics of Zn^{2+}. Additionally, the hybrid interphase facilitates the migration and transport of zinc ions in the SEI, ensures the even distribution of Zn^{2+} on the anode surface, and effectively isolates the zinc anode from water molecules. The synergistic effect of the weakly solvating electrolyte and the meticulously optimized SEI layer enables dense zinc deposition and significant enhancement of corrosion resistance of zinc metal anodes at low temperatures. As a result of the joint effects, with a current density of 0.5 mA/cm^2 and a capacity of 0.5 mAh/cm^2, Zn//Zn symmetric cell can cycle for 1200 h at a low temperature of −40 °C. The Zn//NVO cell achieves an initial discharge capacity of 77.42 mAh/g and an ultra-long cycle lifespan over 1000 cycles with a high capacity retention of 82.89 % at 1 A/g at −40 °C. The remarkable performance achieved underscores the feasibility of the weakly solvating electrolyte with interphase design effect in addressing concerns related to cycle life and the challenges of low-temperature operation.

A series of DMS/water hybrid electrolytes with 1 mol/L $Zn(OTf)_2$ were prepared (Fig. S1 in Supporting information). The volume ratio of DMS was increased from 0 %, 30 %, 50 %, 70 %, to 100 %, and the corresponding electrolyte is labeled as Water, W7D3, W5D5, W3D7 and DMS, respectively. Density functional theory (DFT) was employed to analyze the interactions between DMS and water, as depicted in Fig. 1a. The calculated binding energy for the DMS-H_2O (−0.376 eV) was notably higher compared to the H_2O–H_2O interaction (−0.166 eV), which suggests a strong coordination between the oxygen atom in DMS and the hydrogen atoms in H_2O [22]. This interaction effectively weakens the hydrogen bonds among water molecules, leading to a reduction in the freezing point of the hybrid electrolyte. The impact of DMS on the hydrogen-bonding network was further validated through nuclear magnetic resonance (NMR) and Raman spectroscopies. The ^2H NMR spectroscopy illustrated in Fig. 1b reveals the influence of DMS on the water molecules within the hybrid electrolyte. Given the molecular structure and charge distribution, both H_2O and DMS molecules exhibit high polarity. In an aqueous electrolyte system, the more electronegative H_2O molecules tend to attract the shared electron pair, resulting in an asymmetric charge distribution [23]. This phenomenon leads to the formation of dipoles,

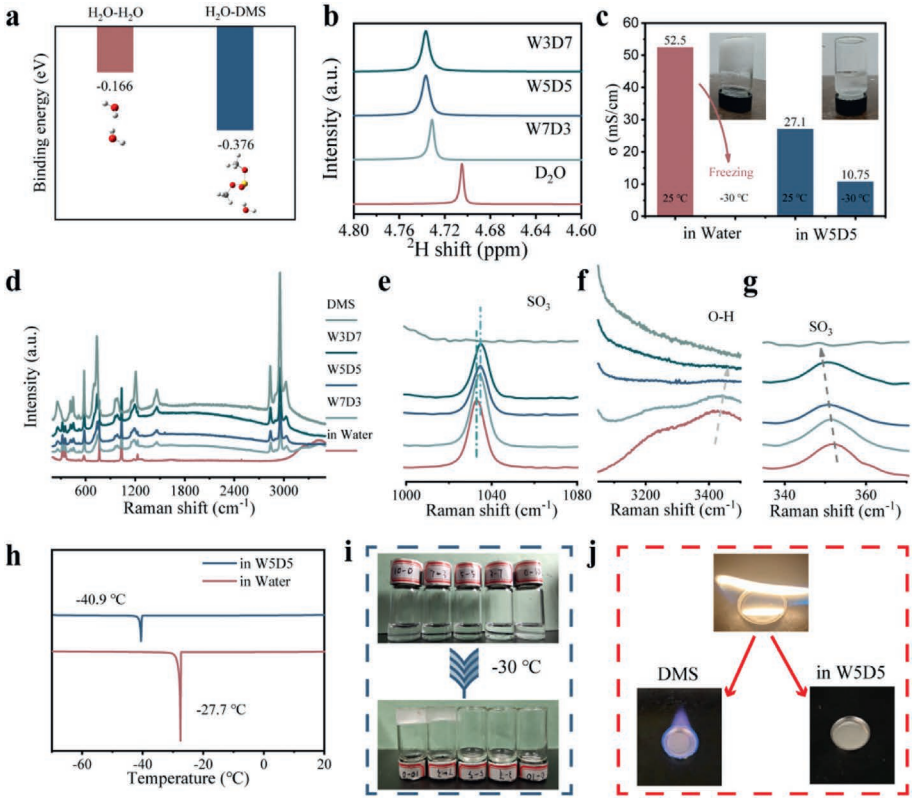


Fig. 1. (a) The calculated binding energy of Zn^{2+}-H_2O and Zn^{2+}-DMS. (b) ^2H NMR spectra of different electrolytes. (c) Ionic conductivities of different electrolytes at different temperatures. (d-g) Raman spectra of different electrolytes. (h) DSC curves of different electrolytes to obtain the freezing points. (i) The photographs of different electrolytes at 25 °C (top) and −30 °C (bottom). (j) Combustion tests of pure DMS and composite electrolyte.

establishing polar bonds between H_2O and DMS molecules. Accordingly, when DMS is introduced to water at varying molar ratios, it anchors a certain proportion of free water molecules. Notably, the ^2H signal of H_2O gradually shifted to a low field with the increase of DMS. Raman spectroscopy (Fig. 1d), which is notably responsive to fluctuations in molecular dipole moments, was utilized to ascertain the mechanism how DMS molecules attenuate the solvation interactions between Zn^{2+} ions and water molecules. Figs. 1e–g and Fig. S2 (Supporting information) display the typical vibration peaks (sulfonate group -SO_3 and -CF_3 group) of $Zn(OTf)_2$. A strong band observed in the Raman spectra at ~3410 cm^{-1} is attributed to the free -OH stretching vibrations of water molecules [24]. It is noteworthy that the -OH stretching vibrations in the electrolyte undergo a slight blue shift upon the introduction of DMS at varying concentrations. This spectral shift implies that the interactions among H_2O molecules are diminished within the DMS-H_2O solvent. Furthermore, the shift of the -SO_3 and -CF_3 groups provides additional evidence that both DMS and the OTf^- anions enter into the solvation shell of Zn^{2+}, subsequently displacing partial water molecules. These findings underscore that DMS is capable of interacting with water, leading to the reformation of hydrogen bonds in water. Concurrently, the hybrid electrolyte can exhibit a reduced freezing point and enhanced ionic conductivity at low temperatures, which is pivotal for its performance in cold-weather applications. Apart from these chemical properties, the influence of DMS concentration on the stability of Zn metal anode was also investigated to determine optimum electrolyte. Clearly, Zn//Zn symmetric cell with W5D5 hybrid electrolyte outperform those with W7D3 and W3D7 in terms of cycle stability (Figs. S3 and S4 in Supporting information). Therefore, it is concluded that the optimum electrolyte is determined to be W5D5 (1 mol/L $Zn(OTf)_2$ in DMS/water hybrid solution (5:5, v/v). Furthermore, the low-temperature behaviors of different electrolytes are investigated. High ionic conductivity is crucial to the application of low-temperature AZIBs. The ionic conductivities of different electrolytes were measured at the temperature of 25 and −30 °C.

As shown in Fig. 1c, pristine electrolyte shows a higher ionic conductivity of 52.5 mS/cm than that of W5D5 electrolyte (27.1 mS/cm) at 25 °C, which may result from the viscosity increasement with the addition of DMS. However, when the temperature drops to −30 °C, the original electrolyte has frozen and the conductivity cannot be measured. Conversely, W5D5 electrolyte remains liquid and exhibits a conductivity of up to 10.75 mS/cm. Apart from ionic conductivity, the destruction of hydrogen bonds by the DMS can effectively lower the freezing point of the electrolyte [25]. According to differential scanning calorimetry (DSC) (Fig. 1h), original electrolyte was frozen at −27.7 °C, whereas the temperature at which the solid-liquid transition occurs in W5D5 electrolyte reaches −40.9 °C. Besides, optical images of the electrolytes with varying DMS concentrations at both 25 and −30 °C (Fig. 1i) reveal that all electrolytes remain in a liquid state at room temperature. However, upon cooling to −30 °C, a distinct difference is observed: while the Water and W7D3 electrolytes freeze, W5D5, W3D7 and DMS still remain unfrozen. This observation indicates that the incorporation of DMS into a 1 mol/L $Zn(OTf)_2$ solution significantly enhances the electrolyte's resistance to freezing, thereby endowing it with superior antifreeze characteristics. Taking into account that DMS is a flammable organic solvent, it is imperative to evaluate the combustibility of the W5D5 electrolyte. As depicted in Fig. 1j, the electrolyte remains original state without catching fire after ignition tests, underscoring the high security of the hybrid electrolyte. This finding also implies that the incorporation of DMS into the electrolytes cannot compromise the inherent safety properties of AZIBs.

For aqueous batteries, the cells are prone to failure at temperatures below 0 °C due to the freezing of water molecules, which poses a significant risk to energy storage devices. As shown in Figs. 2a and b and Fig. S5 (Supporting information), the Zn//Zn

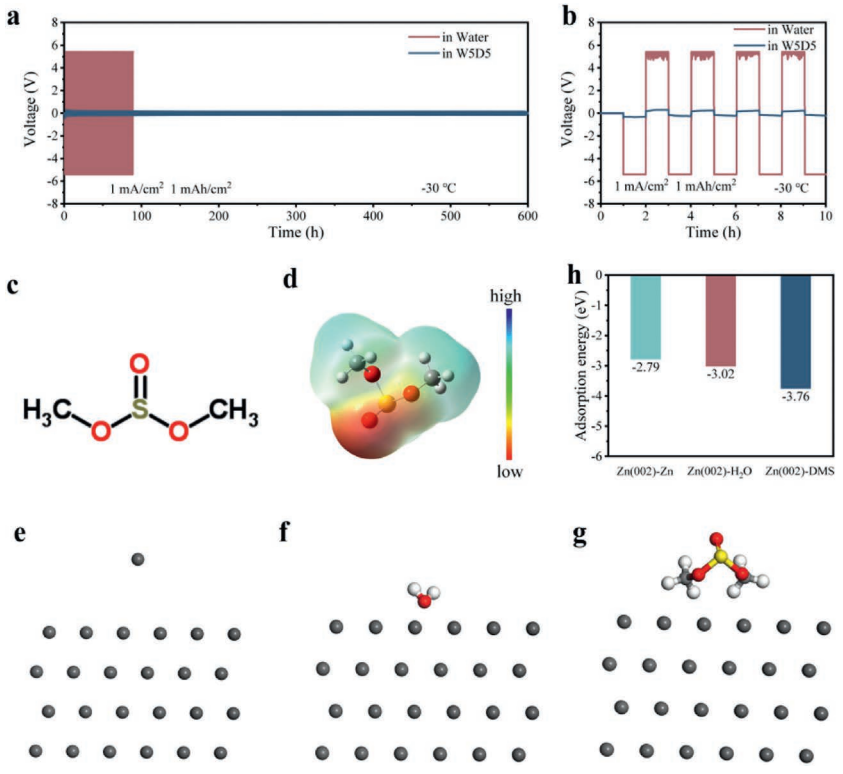


Fig. 2. (a) Voltage-time curves of symmetric cells at −30 °C in 1 mol/L in Water and W5D5. (b) The enlarged voltage profiles of the symmetrical cells. (c, d) Molecular structure and electrostatic potential mapping of DMS. The structures of the (e) Zn atom, (f) water molecule and (g) DMS molecule adsorbed on Zn. (h) The adsorption energy of the Zn atom, DMS molecule and H_2O molecule on the surface of Zn.

symmetric cell using the control electrolyte (1 mol/L $Zn(OTf)_2$ in water) cannot operate properly because the electrolyte has been frozen, and the ion migration and reaction kinetics are extremely slow [26,27]. It is generally believed that electrolyte freezing obstructs ion transport and diminishes interfacial wettability, leading to a substantial decline in the electrochemical performance of cells at low temperatures. Remarkably, the symmetric cell with W5D5 electrolyte exhibits a long lifespan of over 600 h at a current density of 1 mA/cm^2 at −30 °C, which demonstrates the practical feasibility and great potential for the applications of such hybrid electrolyte under low temperature.

The polar sulfinyl group in DMS is highlighted in Fig. 2c, which is a key feature of its chemical structure. Fig. 2d presents the electrostatic potential (ESP) diagram of DMS, showing a concentration of electron density on the oxygen atom within the sulfinyl group (S=O). The high electronegativity of O coupled with the lone pair, creates an electron-withdrawing effect, which can provide nucleophilic sites and enable it to interact effectively with Zn^{2+} ions and water molecules [28,29]. This suggests that DMS preferentially adsorbs on the surface of the electrode, promoting the reorganization of the electric double layer (EDL). To substantiate this hypothesis, density functional theory (DFT) calculations were performed to analyze the adsorption interactions between DMS and Zn metal anodes. These calculations assessed the interaction ability of various molecules for the Zn anode. The optimized adsorption structures are depicted in Figs. 2e–g, with the corresponding calculation results presented in Fig. 2h. The calculated adsorption energy for DMS (−3.76 eV) is significantly lower compared to H_2O (−3.02 eV), signifying a much stronger adsorption behavior of DMS on the Zn (002) crystal plane [30,31].

The adsorption behaviors of DMS and compositions in SEI on Zn anode surface during cycling were explored. From the scanning electron microscopy (SEM) images and energy dispersive spectrometry (EDS) elemental maps in Fig. 3a, uniform distribution of Zn, S, and F are detected on the surface of cycled Zn anode [32]. X-ray photoelectron spectroscopy (XPS) coupled with Ar ion sputtering was utilized to investigate the depth profile of the SEI components on the Zn surface. Figs. 3b–d illustrate that the initial SEI layer (prior to sputtering) is notably enriched with ZnS species and inorganic ZnF_2. Drawing from previous studies, the presence of ZnF_2 arises from the partial reduction of OTf^- ions, while the -CF_3SO_3 group stems from residual salt on the Zn surface. The ZnS species can be attributed to the result of the decomposition of Zn^{2+}-DMS complexes. As sputtering progresses, the peak intensity of ZnF_2 notably intensifies, whereas the peak intensity of ZnS remains relatively stable with no significant fluctuations. After 40 nm of sputtering, the predominant constituents of the SEI are a blend of ZnF_2 and ZnS. The XPS analyses robustly indicate that the W5D5 electrolyte promotes the *in situ* formation of a hybrid interlayer on the Zn surface [33]. This hybrid SEI, in contrast to the unstable SEI layer formed by the pristine electrolyte, enriches the interface between the SEI and Zn metal with Zn^{2+} species and enhances the transport of Zn^{2+} ions from the electrolyte to the metal. This enhancement significantly contributes to the stable operation of the battery at low temperatures. The mechanisms and effects are illustrated in Fig. 3e.

The exceptional stability of AZIBs at subzero temperatures strongly suggests that temperature plays a pivotal role in interphase evolution, even with identical electrolyte components [34]. The electrochemical stability window (ESW) of aqueous electrolytes is typically constrained by hydrogen and oxygen evolution reactions [35,36]. Consequently, we conducted a thorough evaluation of the ESW for the W5D5 electrolyte at different temperatures using linear sweep voltammetry (LSV), as depicted in Figs. 4a–c.

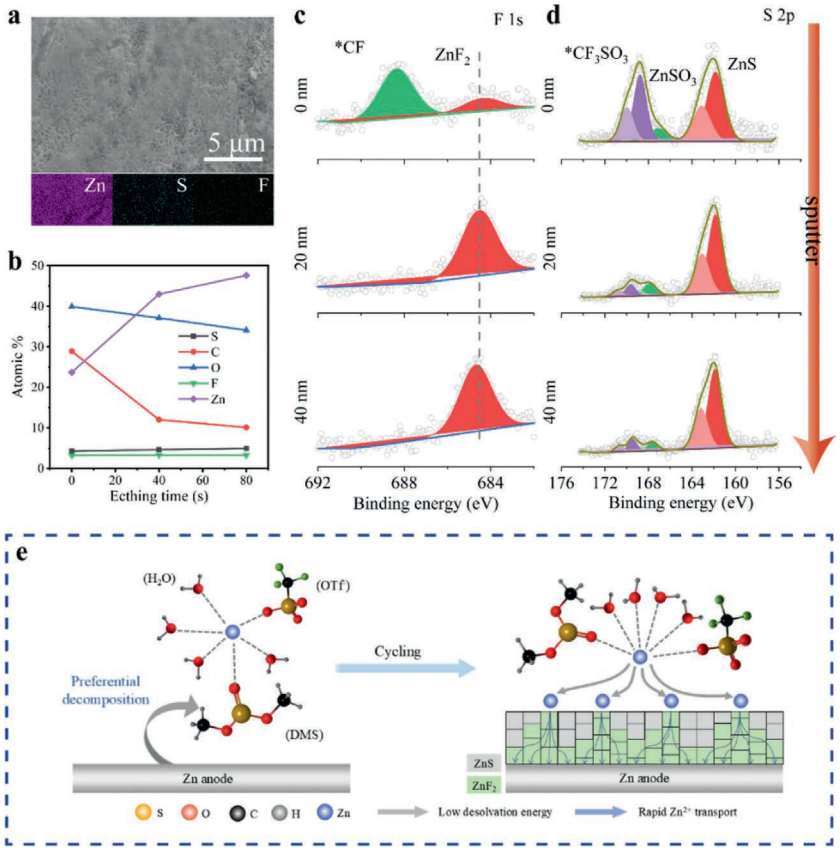


Fig. 3. (a) SEM images and corresponding EDS spectrum of Zn electrode in composite electrolyte cycling for 20 cycles. (b–d) In-depth XPS spectra on the Zn anode after 20 cycles in composite electrolyte. (e) Schematic illustration of formation process and action mechanism about hybrid interphase.

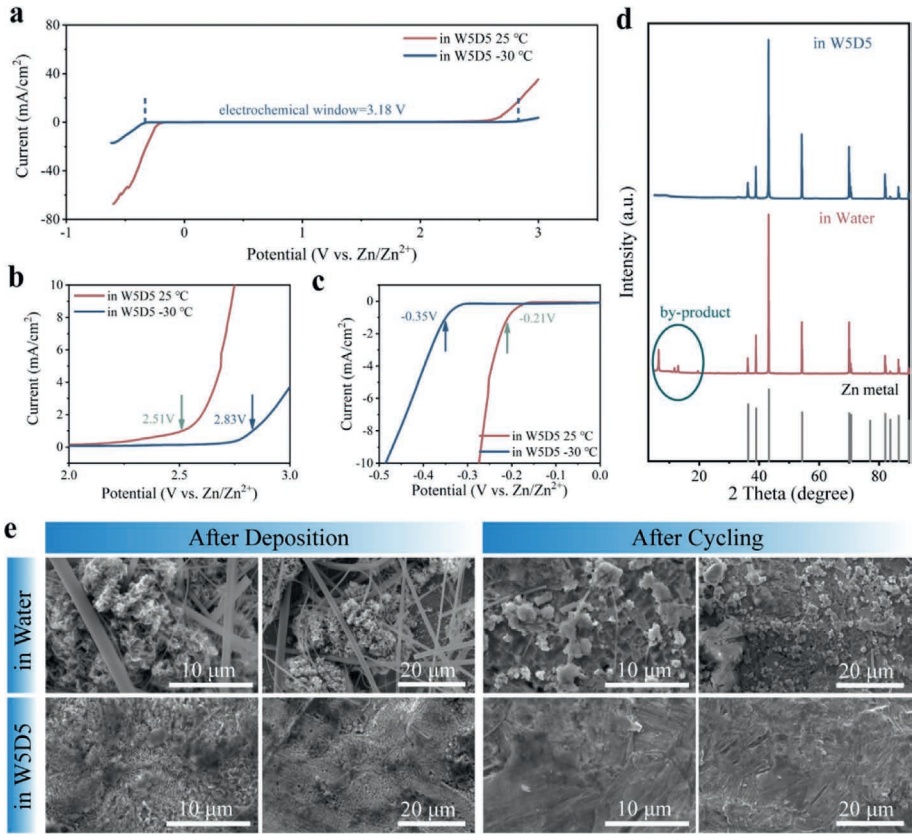


Fig. 4. (a–c) The electrochemical window of composite electrolyte measured using polarization scanning on non-active Ti electrodes under different temperatures. (d) XRD pattern of Zn sheets after 50 cycles in different electrolytes. (e) SEM characterizations of Zn anode surface using different electrolytes after deposition and 20 cycles at −30 °C.

Specifically, the investigation reveals that a low-temperature environment significantly lowers the onset potential for the HER from −0.21 V to −0.35 V (*versus* Zn/Zn^{2+}). Concurrently, the onset potential for the oxygen evolution reaction (OER) is elevated, increasing from 2.51 V to 2.83 V. Overall, this results in an electrochemical window of approximately 3.18 V for the W5D5 electrolyte at −30 °C, which is substantially wider than that observed at room temperature (25 °C), exhibiting that DMS molecules could efficiently reduce the activity of water and improve the electrochemical stability of the aqueous electrolyte, especially at low temperatures.

Generally, the intensified HER raises the local pH, consequently triggering zinc corrosion and the formation of by-products [37–39]. The passivation by-products accumulated on the surface of the zinc electrode will block the electron/ion migration on the electrode surface and further exacerbate dendrite growth. Thus, X-ray diffraction (XRD) analysis (Fig. 4d) was conducted to investigate the formation of by-products on Zn electrodes after 50 cycles in different electrolytes. The XRD patterns at room temperature reveal distinct diffraction peaks, signifying the presence of by-products. In stark contrast, the XRD patterns exhibit negligible peaks associated with by-products on the surface of Zn anodes cycled in the W5D5 electrolyte, reflecting the inhibition effect of DMS on surface corrosion [40,41]. Apart from the improvement in inhibiting HER, the by-products formation, and corrosion issues, the W5D5 electrolyte is believed to be also capable of improving Zn plating/stripping reversibility. The morphology of the Zn anode after initial plating and subsequent cycling cycles can elucidate the influence of DMS on Zn deposition. The corresponding SEM images are presented in Fig. 4e. With DMS modification, Zn deposits after plating are notably dense and smooth. After 20 cycles, these deposits retain their initial morphological characteristics without Zn dendrite and holes, suggesting that the hybrid SEI layer can efficiently inhibit the growth of Zn dendrites during the repeated Zn plating/stripping process. In contrast, at low temperatures, Zn deposition in the unmodified electrolyte leads to dendritic growth due to hindered charge transport and a sluggish desolvation process. The formation of mossy Zn deposits and flake-like by-products are found after initial deposition and subsequent 20 cycles in the blank electrolyte. Therefore, we conclude that the weakly solvating electrolyte coupled with robust hybrid interphase can significantly suppress water-induced side reactions, mitigate Zn corrosion, and prevent the growth of Zn dendrites. This synergistic effect enhances the cycling stability of Zn anodes and ensures the stability of AZIBs under practical and harsh conditions.

To evaluate the practical use of the W5D5 electrolyte, symmetrical and full batteries with different electrolytes were assembled and tested. Impressively, the symmetrical cell with W5D5 electrolyte can stably cycle for 1200 h at 0.5 mA/cm^2 despite temperature as low as −40 °C (Fig. 5a). In sharp contrast, the cell in blank electrolyte fails to achieve stable operation (Fig. 5b) due to the freeze of bare electrolyte, reduced interfacial wettability and low reaction kinetic [42]. Notably, there was essentially no change in voltage polarization of the symmetrical cell with W5D5 electrolyte upon cycling (Fig. 5c), suggesting invariant charge-transfer resistance [43]. Furthermore, full cells were constructed with Zn foil serving as the anode and NVO as the cathode. NVO, a common cathode material, is known for its straightforward preparation process and its reliable performance during charging/discharging processes. At −40 °C, the initial capacity of this full cell in W5D5 electrolyte at 1 A/g is 77.42 mAh/g, and an ultra-long cycle lifespan over 1000 cycles with a high capacity retention of 82.89 % is achieved (Figs. 5d and e). In addition, the surface morphology of Zn anodes after 50 cycles at 1 A/g was obtained. It can be seen

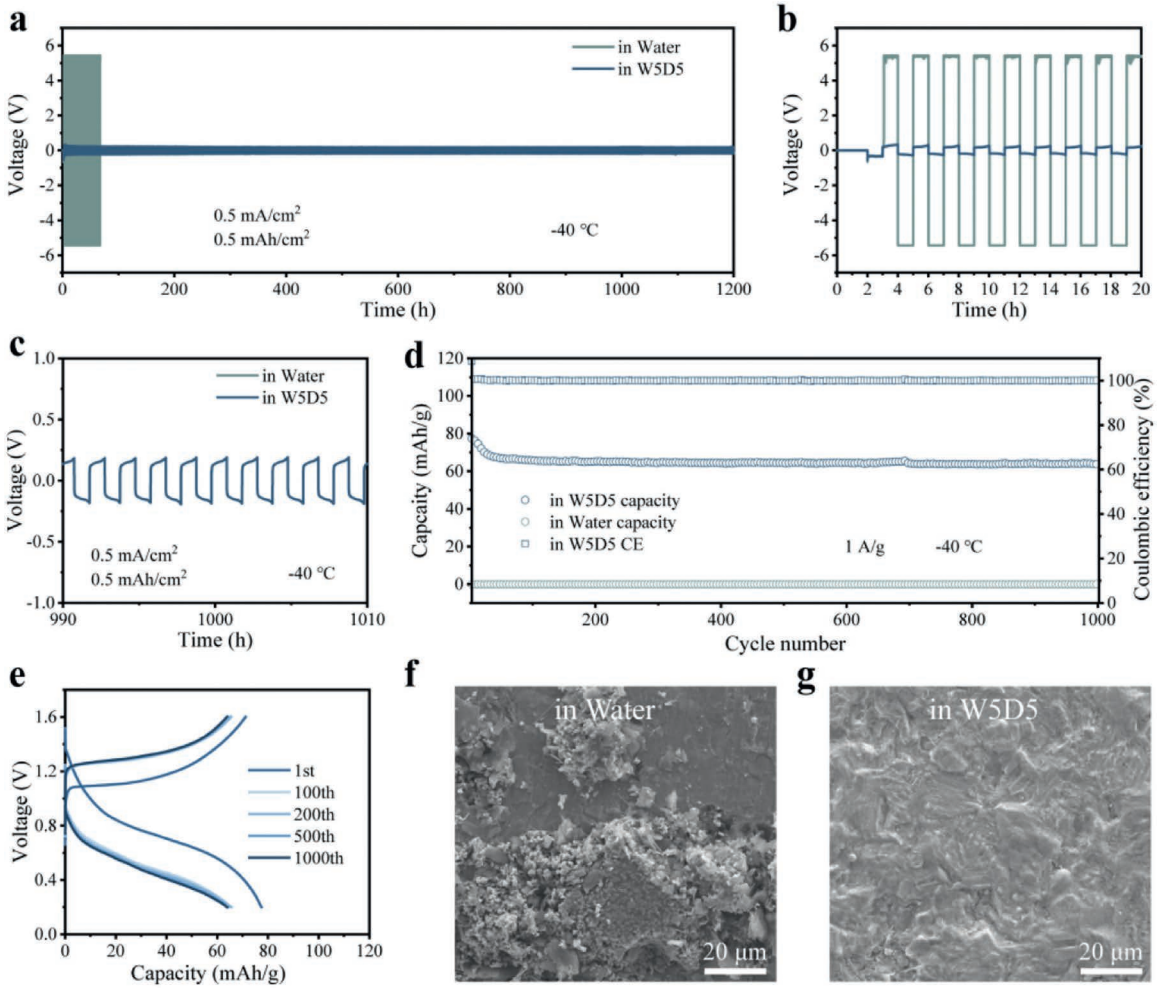


Fig. 5. (a–c) Cycling performance of Zn//Zn cells using different electrolytes at 0.5 mA/cm^2 for a capacity of 0.5 mAh/cm^2 at −40 °C. (d) The long-term cycling performance of Zn//NVO cells with different electrolytes at −40 °C. (e) Selected GCD curves. SEM images of Zn anode surface cycled in (f) Water and (g) W5D5 electrolytes for 50 cycles.

that many disorderly dendrites and mossy Zn deposits are formed on the zinc surface cycled in blank electrolyte (Fig. 5f). Conversely, under the protection of the DMS induced interfacial layer, the Zn anode cycled in W5D5 electrolyte maintains a compact and denser deposition morphology without corrosion pits (Fig. 5g). These results demonstrate that such weakly solvating electrolyte induced hybrid interphase is a remarkably promising strategy to stabilize Zn metal electrodes in extreme low-temperature environments.

A low-temperature electrolyte obtained by introducing DMS into the aqueous electrolyte for use in AZIBs is well fabricated. First, DMS effectively disrupts the hydrogen-bonding network of water, achieving a remarkable reduction in the freezing point of electrolyte to −40.9 °C. DMS also boosts the ionic conductivity, which impressively reaches 27.1 mS/cm at 25 °C and 10.75 mS/cm even at −30 °C. Second, DMS and OTf^- involved solvated structure is easier to desolvate, and DMS is more likely to adsorb on the Zn anode surface compared with water. Third, the distinct chemical reactivities of DMS cosolvent and OTf^- anions have led to the successful creation of a ZnF_2-ZnS hybrid SEI, which can facilitate Zn^{2+} desolvation and achieve fast Zn^{2+} conduction. The weakly solvating electrolyte and the well-optimized SEI layer can synergistically suppress dendrites, HER, and by-products, leading to continuous cycling under cold environments. Remarkably, the Zn symmetric cells reach superior stability at −40 °C with a lifespan of 1200 h at 0.5 mA/cm^2. Besides, the Zn//NVO cell delivers a high initial capacity of 77.42 mAh/g at 1 A/g over 1000 cycles at −40 °C. This work provides a feasible path to achieve high-performance AZIBs under extreme conditions from the perspective of the weakly solvating electrolyte with interphase design regulation.

Declaration of competing interest

The authors declare that they have no known competing financial interests or personal relationships that could have appeared to influence the work reported in this paper.

CRediT authorship contribution statement

Wen Liu: Writing – original draft, Data curation, Conceptualization. **Qiwen Zhao:** Methodology, Investigation. **Hongli Qi:** Software, Methodology. **Dongping Chen:** Formal analysis, Data curation. **Fengcheng Tang:** Investigation, Formal analysis. **Xiaoyu Liu:** Visualization, Validation. **Huaming Yu:** Writing – review & editing, Visualization, Supervision. **Gang Zhou:** Writing – review & editing, Supervision, Project administration. **Yuejiao Chen:** Supervision, Resources, Project administration. **Libao Chen:** Writing – review & editing, Validation, Project administration.

Acknowledgments

This research was financially supported by the National Natural Science Foundation of China (No. 52377222) and Natural Science Foundation of Hunan Province (No. 2023JJ20064).

Supplementary materials

Supplementary material associated with this article can be found, in the online version, at doi:10.1016/j.cclet.2025.110893.

References

[1] S. Huang, K. Li, Z. He, et al., J. Alloy. Compd. 1005 (2024) 176193.
[2] Y. Zhong, C. Cao, L. Zhao, M.O. Tadé, Z. Shao, Green Carbon 2 (2024) 94–100.
[3] D. Sun, Z. Sun, D. Yang, et al., EcoEnergy 1 (2023) 375–404.
[4] H.M. Yu, C.D. Lv, C.S. Yan, G.H. Yu, Small Methods 8 (2024) 2300758.
[5] W.D. Zhang, C. Sun, Y.X. Zhu, F. Gao, C. Lai, Rare Met. 43 (2024) 3044–3054.
[6] F. Chen, Z.L. Xu, Microstructures 2 (2022) 2022012.
[7] J. Ren, H.Y. Wu, W. Yan, P. Huang, C. Lai, Ind. Chem. Mater. 2 (2024) 328–339.
[8] H. Yang, H.F. Zheng, H.M. Yu, et al., Nanoscale 14 (2022) 13722–13730.
[9] H. Yu, Z. He, D. Chen, et al., Energy Rev. 4 (2025) 100107.
[10] G. Ma, W. Yuan, X. Li, et al., Adv. Mater. 36 (2024) 2408287.
[11] W. Qu, C. Wen, B. Chen, Y. Cai, M. Zhang, Sci.China Mater. 67 (2024) 2889–2897.
[12] D. Tang, X. Zhang, D. Han, et al., Adv. Mater. 36 (2024) 2406071.
[13] M. Cheng, D. Li, J. Cao, et al., Angew. Chem. Int. Ed. 63 (2024) e202410210.
[14] M. Qiu, Y. Liang, J. Hong, et al., Angew. Chem. Int. Ed. 63 (2024) e202407012.
[15] X. Shi, J. Zeng, A. Yi, et al., J. Am. Chem. Soc. 146 (2024) 20508–20517.
[16] J. Zhou, H. Yu, P. Qing, et al., J. Colloid Interface Sci. 678 (2025) 772–782.
[17] C. Li, X. Jiang, H. Qi, et al., Energy Storage Mater. 75 (2025) 104012.
[18] S. Huang, R. Tang, X.Q. Liu, et al., Energy Environ. Sci. 17 (2024) 591–601.
[19] G.M. Qu, H. Wei, S.S. Zhao, et al., Adv. Mater. 36 (2024) 2400370.
[20] W. Song, X. Xie, L. Deng, et al., Energy Storage Mater. 70 (2024) 103489.
[21] X. Guo, G. He, J. Mater. Chem. A 11 (2023) 11987–12001.
[22] R.Z. Zhao, X.S. Dong, P. Liang, et al., Adv. Mater. 35 (2023) 2209288.
[23] X.P. Ma, H.M. Yu, C.S. Yan, et al., J. Colloid Interface Sci. 664 (2024) 539–548.
[24] W. Kong, F. Wan, Y. Lei, et al., Anal. Chem. 96 (2024) 15313–15321.
[25] S.Z. Deng, B.G. Xu, J.X. Zhao, H. Fu, Energy Storage Mater. 70 (2024) 103490.
[26] D.D. Wang, H.L. Peng, S.J. Zhang, et al., Angew. Chem. Int. Ed. 62 (2023) e202315834.
[27] M. Liu, L. Yao, Y. Ji, et al., Nano Lett. 23 (2023) 541–549.
[28] Y.X. Zhao, S. Guo, M.J. Chen, et al., Nat. Commun. 14 (2023) 7080.
[29] C. Zhang, C. Li, D. Chen, et al., J. Colloid Interface Sci. 682 (2025) 232–241.
[30] Y.S. Li, X.D. Yang, Y. He, et al., Adv. Funct. Mater. 34 (2024) 2307736.
[31] S. Zhou, X. Meng, Y. Chen, et al., Angew. Chem. Int. Ed. 63 (2024) e202403050.
[32] L. Wang, H. Yu, D. Chen, et al., Carbon Neutrality 3 (2024) 996–1008.
[33] L.S. Han, Y.M. Guo, F.H. Ning, et al., Adv. Mater. 36 (2024) 2308086.
[34] W. Wang, S. Chen, X. Liao, et al., Nat. Commun. 14 (2023) 5443.
[35] Z. He, H. Yu, M. Fu, et al., Energy Storage Mater. 70 (2024) 103469.
[36] F. Bu, Y. Gao, W.B. Zhao, et al., Angew. Chem. Int. Ed. 63 (2024) e202318496.
[37] N. Hu, W.S. Lv, W.J. Chen, et al., Adv. Funct. Mater. 34 (2024) 2311773.
[38] Y. Liu, H. Fu, C. Gao, et al., Adv. Energy Mater. 15 (2025) 2403562.
[39] H. Yu, D. Chen, L. Zhang, et al., Trans. Nonferrous Met. Soc. China 34 (2024) 3118–3150.
[40] Y. Bai, D. Deng, J. Wang, et al., Adv. Mater. 36 (2024) 2411404.
[41] Q. Zhao, W. Liu, X. Ni, et al., Adv. Funct. Mater. 34 (2024) 2404219.
[42] C. Li, T. Liao, D. Chen, et al., Chin. Chem. Lett. 36 (2025) 110557.
[43] M.Y. Liu, W.T. Yuan, G.Q. Ma, et al., Angew. Chem. Int. Ed. 62 (2023) e202304444.